# Adsorption and charge transfer dynamics of bi-isonicotinic acid on Au(111)

J. Ben Taylor, Louise C. Mayor, Janine C. Swarbrick, and James N. O'Shea[a)]
*School of Physics and Astronomy, University of Nottingham, Nottingham NG7 ZRD, United Kingdom*

Cristina Isvoranu and Joachim Schnadt
*Department of Synchrotron Radiation Research, Lund University, Box 117, S-22100 Lund, Sweden*

(Received 18 April 2007; accepted 16 August 2007; published online 2 October 2007)

The interaction of bi-isonicotinic acid (4,4′-dicarboxy-2,2′-bipyridine) with the Au(111) surface has been investigated using electron spectroscopic techniques. Near edge x-ray absorption fine structure (NEXAFS) spectra show that monolayers of the molecule lie flat to the surface and also reveal that the monolayer is sensitive to the preparation conditions employed. Core level x-ray photoelectron spectroscopy (XPS) shows that the adsorbed molecule does not undergo deprotonation upon adsorption. The "core-hole clock" implementation of resonant photoemission has been used to probe the coupling between molecule and substrate. This technique has revealed the possibility of ultrafast backtransfer from the substrate into the molecule upon resonant excitation of a N 1*s* core level electron. This is supported by a NEXAFS and XPS investigation of energy level alignments in the system. © *2007 American Institute of Physics*. [DOI: 10.1063/1.2781510]

## I. INTRODUCTION

Bi-isonicotinic acid or 4,4′-dicarboxy-2,2′-bipyridine ("dcb") shown in Fig. 1, forms the ligand groups through which many technologically important dye molecules anchor to model solar cell surfaces. One of the most notable examples is that of "N3" $[(dcb)_2Ru(NCS)_2]$. This dye molecule is used in the Grätzel dye-sensitized solar cell (DSSC),[1,2] which operates on the principle of sensitizing films of interconnected $TiO_2$ colloids. Such cells are currently being manufactured and offer a credible alternative to inorganic devices.

Study of the adsorbate-substrate interface is particularly important in the search for better DSSCs. This is evident from the way in which charge carriers are generated in DSSCs, as opposed to inorganic photovoltaics (IPV). In IPVs photons are absorbed to create pairs of free electrons and holes. These pairs are created spatially coincident in the same phase and require an electric field to drive charge separation. In DSSCs photon absorption results in the generation of excitons rather than free carriers. Free carriers are only created upon dissociation over a phase boundary, whereby they are already spatially separated. In this way, the photovoltage of DSSCs are not fundamentally dependent on internal electrical potential gradients but are more influenced by the chemical potential gradients of the charge carriers.[3] A proper understanding of the geometry and carrier dynamics at the interfaces of DSSCs is therefore crucial for the evolution of such cells.

However, spectroscopic study is often limited by the fragile nature of the dyes, prohibiting sublimation techniques used in ultrahigh vacuum surface preparation. Alternative "wet" preparations can be highly complicated when performed *in situ* and are more difficult to minimize contaminants. Thus, the "next best" molecules to study are those of the binding ligands. These give a measure of how the full dye will interact with the surface.[4–6]

Motivation for the specific system choice comes from the recent DSSC developed by McFarland and Tang.[7] Their cell consists of the four layers $Ti/TiO_2/Au/dye$. It was proposed that, following photoexcitation of the dye, electrons are injected into the $TiO_2$ layer via ballistic passage through an ultrathin Au film, which ranges in thickness from 15 to 50 nm. The Au layer then scavenges the holes left behind in the dye layer. A photovoltage is thus formed by contact between the Au film and the Ti backplate. A merbromin dye on a $Ti/TiO_2/Au$ multilayer was found to give an open-circuit voltage of 600–800 mV and a short-circuit current of 10–18 $\mu A\ cm^{-2}$ at an efficiency of $<1\%$. Although this is low, it was also found that 10% of the adsorbed photons gave rise to an electric current.[7,8] This relatively high internal quantum efficiency, coupled with the fact that the cell has

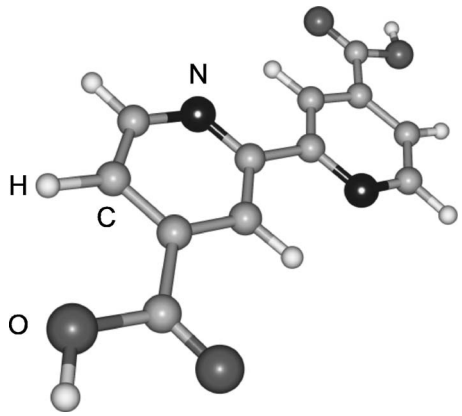


FIG. 1. Bi-isonicotinic acid molecule. Small light spheres represent hydrogen, medium gray spheres represent carbon, large dark gray spheres represent oxygen, and large black spheres represent nitrogen. The geometry is planar and is representative of the gas phase.

[a)]Electronic mail: james.oshea@nottingham.ac.uk

 

been simplified, as compared to other DSSCs, by not needing an electrolyte, makes the cell of interest. Study of the interaction between the Au(111) surface and aromatic carboxylic acids, such as bi-isonicotinic acid, is a first step toward understanding this type of device.

## II. METHOD

Experiments were carried out at the Swedish synchrotron facility MAX-lab in Lund. Beamline I311 (Ref. 9) was used which has a photon energy range of 30–1500 eV and is equipped with a Scienta SES200 hemispherical analyzer. The radiation has a high degree of elliptical polarization and may be considered as linearly polarized. The base pressure in the analysis chamber was in the mid-$10^{-11}$ mbar range and that in the preparation chamber was in the low $10^{-10}$ mbar range.

The substrate was a single crystal Au(111) of dimensions 10 mm diameter $\times$ 2.5 mm (Metal Crystals and Oxides Ltd., Cambridge, UK). It was mounted on a loop of tungsten wire (0.5 mm) that passed tightly through the body of the crystal, ensuring that a good electrical and thermal contact was made. A thermocouple was also attached 2 mm into the crystal in order to monitor the temperature accurately. The crystal was cleaned along the lines of Barth *et al.*[10] by cycles of sputtering using 1 kV Ar ions and then annealing at 900 K by passing a current through the tungsten wire mount. Cleanliness was checked by monitoring the disappearance of the C 1*s* core level. It is noted that although the signal was never reduced to zero, it accounted for less than 5% of the intensity of a monolayer.

Bi-isonicotinic acid (Sigma-Aldrich, UK) was evaporated from a homebuilt evaporator ~20 cm from the sample. The powder was outgassed thoroughly and evaporated at a temperature of ~230 °C. Two preparation methods were tested in forming monolayers of bi-isonicotinic acid. The first type, termed *hot*, involved the initial formation of a multilayer, made by depositing onto the substrate at room temperature. This was then gently heated off at a temperature of ~140 °C until no change was observed in the valence band spectra. This is in line with previous preparations made in the case of a rutile $TiO_2$(110) substrate where bi-isonicotinic acid self-terminated at a monolayer when deposited onto a hot substrate.[11,12] The second type of preparation, termed *cold*, was performed by depositing the acid for a short length of time to form the monolayer directly at room temperature. The thickness of the film was checked by monitoring the valence band as compared to the *hot* preparation technique.

Monochromator exit slits were set to give a resolution of ~100 meV for photons of energy $h\nu$=400 eV. The monochromator was calibrated from the separation between first and second order Au 4*f* peaks. For the recording of NEXAFS and resonant photoemission spectra, a taper (+4 mm) was applied to the undulator to reduce the intensity variation of the radiation as the photon energy was scanned. For these measurements the analyzer pass energy and entrance slits were set to give an analyzer resolution of ~750 meV and hence a total energy resolution (with respect to binding energy) of ~760 meV. The analyzer was also set to record spectra in fixed mode. These settings were found to give the best compromise between energy resolution and the large number of counts required for quantitatively analyzable resonant spectra. For core level spectra, the analyzer was set to give a total energy resolution varying from <150 meV for spectra taken at $h\nu$<350 eV to ~240 meV at $h\nu$=650 eV. For these spectra, the analyzer was set to record in swept mode.

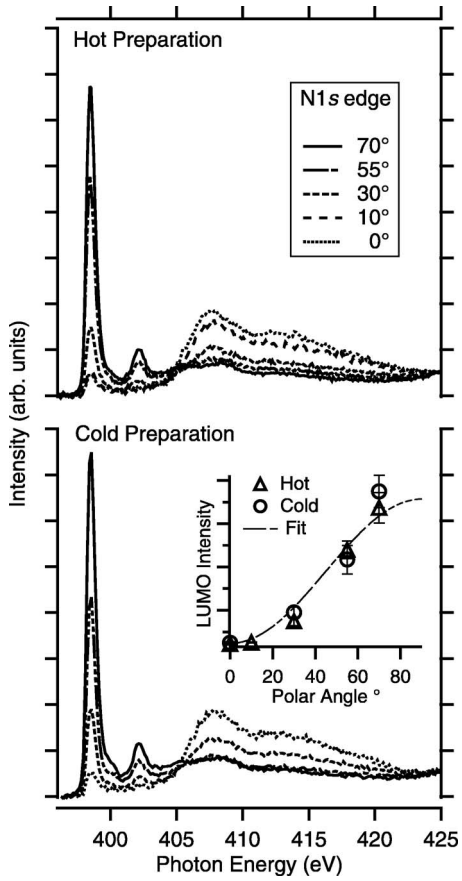


FIG. 2. Angle resolved NEXAFS spectra for the hot and cold preparation methods. Inset shows the variation of the LUMO intensity with the angle of the incident radiation to the surface normal. The fitted curve is the theoretical angular dependence for an aromatic ring with tilt angle of 70° to the surface normal, assuming a random azimuthal orientation and linear light polarization (Refs. 14 and 15). Photon resolution was ~100 meV.

## III. RESULTS

Angle resolved NEXAFS spectra over the N 1*s* edge, for the two preparation techniques, are shown in Fig. 2. The spectra have been corrected for undulator intensity variations and normalized to the continuum of states above the vacuum level (>425 eV).[4,11,13] The angles quoted are those between the surface normal and the wave vector of the radiation. This corresponds to that made by the (dominant component of) electric field vector to the surface plane. Only polar angles were considered as the substrate has a sixfold rotational symmetry, eliminating azimuthal intensity variations.[14,15] The sharp low energy peaks (<406 eV) are identified with the $\pi^*$ unoccupied molecular orbitals. The higher energy structure (>406 eV) is identified with the $\sigma^*$ states.[4,5,12,13]

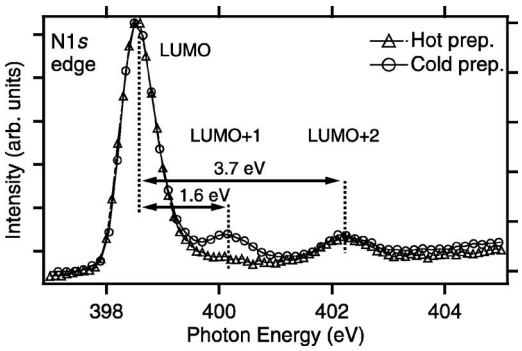


FIG. 3. Higher resolution NEXAFS spectra, over the $\pi^*$ region, for the hot and cold preparation methods. Spectra were taken at normal emission. Photon resolution was ~100 meV.

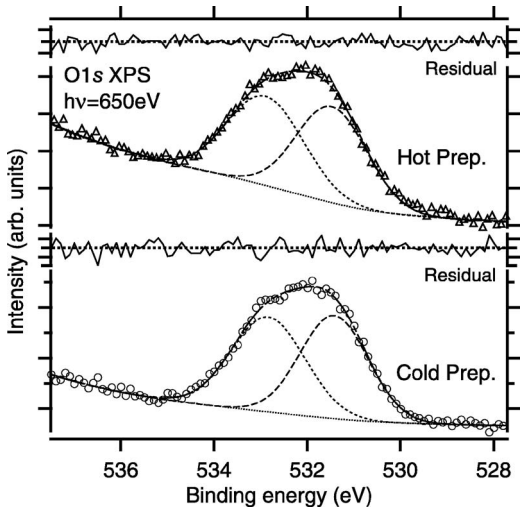


FIG. 4. O 1*s* core level spectra, taken at $h\nu$=650 eV, for the hot and cold preparation methods. Spectra were taken at normal emission. Binding energy is calibrated to the Fermi level of the substrate. Total instrumentation resolution was ~240 meV.

The angle resolved spectra allow information on the orientation of the molecule to be extracted. The dipole matrix element associated with excitation to the $\pi^*$ orbitals is oriented perpendicular to the plane of the aromatic ring structure of the molecule (see Fig. 1). Thus, according to the functional form of the NEXAFS cross section,[14,15] the signal arising due to the core-hole decay from the $\pi^*$ states will be maximized when the polarization vector of the light lies perpendicular to the molecular plane (parallel to the matrix element). The reverse is true of the intensity variation of the $\sigma^*$ states.[14,15]

The strong angular dependence exhibited in Fig. 2 shows that the molecule has a high degree of ordering on the surface. Maximal $\pi^*$ intensity is observed to occur for the electric field perpendicular to the plane of the surface, with minimal intensity for the field oriented in the parallel direction. This is a necessary but insufficient condition that the molecular plane lies flat to the surface. An analysis of the lowest unoccupied molecular orbital (LUMO) intensity variation as a function of angle[14,15] reveals that the plane of the aromatic ring structure has an average tilt angle of $70° \pm 5°$ to the surface normal. This acts as a lower estimate for the angle associated with the optimal molecular geometry with respect to the Au(111) surface, as the sample will not have perfect ordering. The theoretical intensity curve for this tilt angle is plotted with the experimental results, in the inset of Fig. 2. This curve is based on the perfect linear polarization of the light and an averaged azimuthal orientation of the ring structure. The "flat" orientation of the molecule on the Au(111) surface is in stark contrast to its upright geometry on $TiO_2$(110), where the tilt angle has been shown[4] to be less than 25°.

The angular dependence of the NEXAFS spectra is identical, within error, for both the preparation techniques. However, closer inspection of the $\pi^*$ region shows that the shapes of the spectra are different. This region is shown in higher resolution in Fig. 3.

For the cold preparation, a feature is observed at ~400 eV. This is substantially reduced if not absent, for the hot preparation. Considering other studies of the molecule where a rutile $TiO_2$(110) substrate was used, a feature lying a comparable distance between the LUMO and LUMO+2 has also been seen. Thick film investigations of the molecule have found a peak originating as a consequence of inequivalent nitrogen atoms through hydrogen bonding interactions between the nitrogen on one molecule and carboxylic oxygen on another.[16] In such a case, the peak is LUMO component shifted by 1.4 eV (Ref. 16) and accompanied by a correspondingly similar shift in the nitrogen core level. No splitting in the N 1*s* level photoemission (PES) spectrum is found in the present case, thus ruling out H bonding as the origin of the LUMO+1 feature here. Monolayer investigations of the molecule (on $TiO_2$) have also found a peak[11,13] lying close to 400 eV. Theoretical calculations attribute its origin as a consequence of bonding to the $TiO_2$ surface.[4,13] The separation of this LUMO+1 peak from the LUMO was experimentally measured as 2.0 eV.[13] This interpretation, adopted as the most likely explanation in the present case, would suggest a difference between the carboxylic groups in the two preparations, indicating some form of bonding through these groups in the cold monolayer. It is noted that the shapes and energetic positions of the LUMO (398.6 eV) and LUMO+2 (402.3 eV) are extremely similar to those measured for monolayers and multilayers adsorbed on a $TiO_2$ substrate.[4,11,13] This would suggest that these molecular orbitals are relatively unperturbed by the gold substrate, despite the molecule lying down on the surface as compared to the more upright geometry exhibited on $TiO_2$.[11]

Core level spectra also provide significant information on the system. Problematic in their analysis was a large secondary electron background from the underlying gold substrate. This was further complicated by the presence of gold Auger features. The strength of the substrate signal meant that even the weaker Auger transitions provided complications to background subtraction. Thus, although all core levels were monitored, only the O 1*s* levels were quantitatively analyzable.

Oxygen 1*s* core levels for the two preparation techniques are presented in Fig. 4. These were taken at a photon energy of $h\nu$=650 eV, for which the substrate signal was found to vary smoothly. Spectra for both preparations show the presence of two peak components. The oxygen atoms in the mol-

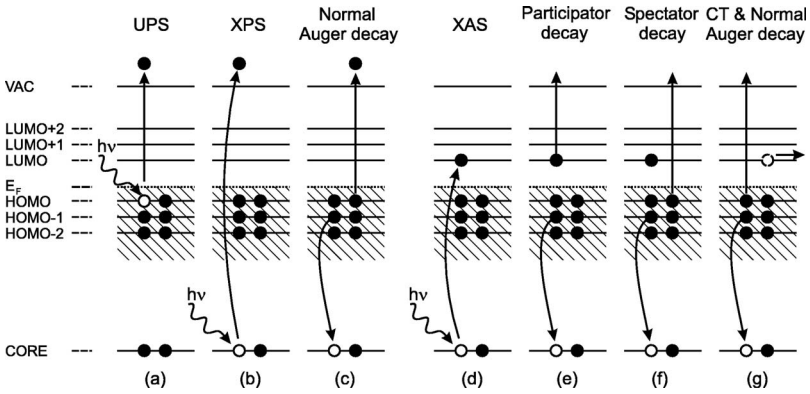


FIG. 5. Electron excitation and deexcitation processes. Spheres represent filled and empty discrete molecular states. Hatched areas represent the valence band of an underlying metallic substrate. (a) Valence band photoemission (UPS), (b) core level photoemission (XPS), (c) Auger decay following core-hole ionization, (d) resonant core level excitation into unoccupied bound states (XAS), (e) participator decay following resonant excitation, (f) spectator decay following resonant excitation, and (g) charge transfer out of unoccupied states and subsequent Auger decay, following resonant excitation.

ecule are therefore in different chemical environments, strongly implying that the molecule does not deprotonate in response to adsorption. This is in contrast to the case of adsorption on a $TiO_2$ substrate.[12]

The spectra were fitted with a combination of an exponential and Shirley background, followed by two Gaussian peak components. Based on the lack of deprotonation, peak components were constrained to have the same spectral weight (area). This is also in line with multilayers on $TiO_2$(110).[12] Unconstrained fits were also made but either resulted in peak components sufficiently similar to the constrained or components that were physically unrealistic. The component at high binding energy (BE) is identified with the hydroxyl oxygen and that at lower energy with the carbonyl oxygen of the molecule.[4,17] It is found that there is no difference between the spectra for the two preparations outside the level of experimental uncertainty. The separation of peak components is $1.42 \pm 0.05$ eV, slightly larger than that found in a multilayer (1.23 eV).[12] This increase in separation reveals an asymmetry to the change in local environment for the two types of oxygen atom, when comparing to the case of a multilayer. The most plausible explanation is a larger decrease in relative BE for the carbonyl oxygen (as opposed to a larger relative increase in BE for the hydroxyl). This would then imply a stronger interaction of the carbonyl oxygen with the Au surface.

The strength of the coupling between bi-isonicotinic acid and the gold substrate can be elucidated through the "core-hole clock" implementation of resonant photoemission spectroscopy (RPES).[5,6,18–21] Processes relevant to this technique are shown in Fig. 5. Molecules are excited through the promotion of core level electrons into unoccupied molecular states. Such molecules can decay via a number of deexcitation channels. Participator decay channels are those Auger deexcitations that involve the electron that was initially excited [see Fig. 5(e)]. Conversely, spectator channels are those that do not involve this electron, with Auger deexcitation proceeding via electrons located in the highest occupied molecular orbitals [see Fig. 5(f)]. When the molecule is coupled to a surface, both of these autoionization channels will compete with charge transfer of the initially excited electron from the unoccupied molecular states into the conduction band of the substrate, followed by normal Auger decay [see Fig. 5(g)], provided that there is a sufficient energetic overlap between the relevant unoccupied orbital and the conduction band states. The important point is that competition occurs on the time scale of the core-hole lifetime, which is typically of the order of femtoseconds. Thus, by monitoring the decay channels, ultrafast charge transfer dynamics can be probed. This implicitly relates to the electronic coupling between the molecules and the substrate as to achieve charge transfer on a femtosecond time scale, there must be a strong electronic wave function overlap between the states involved. For a complete discussion of the technique, the reader is directed to Ref. 20 and the references therein.

A point that has been touched upon, fundamental in addressing the question of whether any interfacial charge transfer occurs in the system, is the *energetics* of the situation. This pertains to the energetic positions of the states potentially involved in the passage of charge between molecular and substrate states. These must be known if the core-hole clock implementation of resonant photoemission is to be used to measure charge transfer times. The energetics is well assessed by the alignment[22] of NEXAFS spectra with valence band spectra (PES). Such results are presented in Fig. 6. Because the substrate is metallic, spectra are referenced to the Fermi level, defined to sit at 0 eV binding energy.

Figure 6 shows that the (core-excited) LUMO+1 and LUMO+2 overlap with unoccupied states in the substrate.

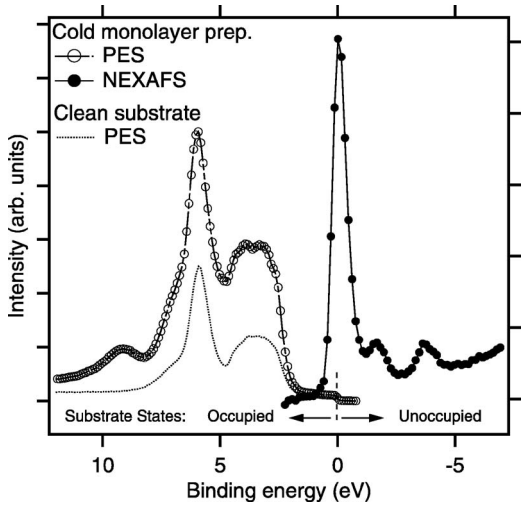


FIG. 6. Energy level alignment of substrate and molecular occupied and unoccupied states. NEXAFS spectrum is over the N 1*s* edge. Spectra were taken at normal emission. Binding energy is calibrated to the Fermi level of the substrate. The sample was prepared using the cold technique.

Thus, charge transfer from these molecular states (after resonant excitation) into the substrate is possible. The situation is more complicated with the LUMO. This is located at the Fermi level of the gold (0 eV). Charge transfer will only be allowed from those vibrational levels located within the lower BE side of the orbital and disallowed from those located to higher BE. It is unlikely that there is charge transfer into the LUMO from the substrate prior to the excitation process. The effect of a positive core hole on the unoccupied orbitals is to shift them to higher binding energy.[5] Before the creation of a core hole, the LUMO will lie at a lower binding energy to that shown in Fig. 6. The magnitude of such a shift can be estimated from the difference between the LUMO binding energy as referenced to the vacuum level (through the core-level ionization potential) and the electron affinity. For the related molecule of pyridine, this gives an estimate[23] of 5.5 eV. Thus, the ground state LUMO will lie above (more negative BE) the Fermi level of the Au. It is noted that the polarization of the metallic substrate has not been taken into account in this estimate. This is justified as screening from conduction band electrons in the substrate is not expected to be significant in a bound state transition for which the molecule will remain neutral.[14]

Figure 7 shows the autoionization spectrum, over the N 1*s* edge, taken for the cold monolayer preparation. Deexcitation channels sit on a constant direct photoemission background from valence states (see Fig. 5). This background is relatively strong as a consequence of both the metallic Au substrate and the analyzer position, relative to the incoming radiation, which promotes the direct PES signal. Participator and spectator deexcitation channels can be identified by their differing dispersion behaviors. Participator channels will leave the system in an identical final state to valence band photoemission (see Fig. 5). This channel will therefore disperse linearly with binding energy. By this, it is meant that as the photon energy is scanned across the resonances, participator electrons remain at a constant BE. In comparison, spectator channels will leave the system in a final state similar to that left by normal Auger decay (following core level ionization). This channel will then disperse linearly with the kinetic energy. It is noted that the bandwidth of the photons used in this experiment is large relative to the bandwidth of the electronic energy levels; thus, resonant photoemission is being conducted outside of the Auger resonant Raman (ARR) regime.[19,20] Operation within this regime was not attempted as the separation between normal Auger and spectator channels is too small to allow a successful identification based on their differing ARR dispersion behavior.

In the current work, it is only the participator channels that are used in the assessment of ultrafast charge transfer. Any reduction in the intensity of the participator signal for the molecule adsorbed on Au(111), as compared to that exhibited by multilayers of the molecule (where ultrafast charge transfer is highly unlikely to occur), can be attributed to the ultrafast charge transfer from the molecule to the Au(111) following resonant excitation of core level electrons. The exact amount of reduction then provides a quantitative handle for extracting charge transfer times and assessing coupling strength.

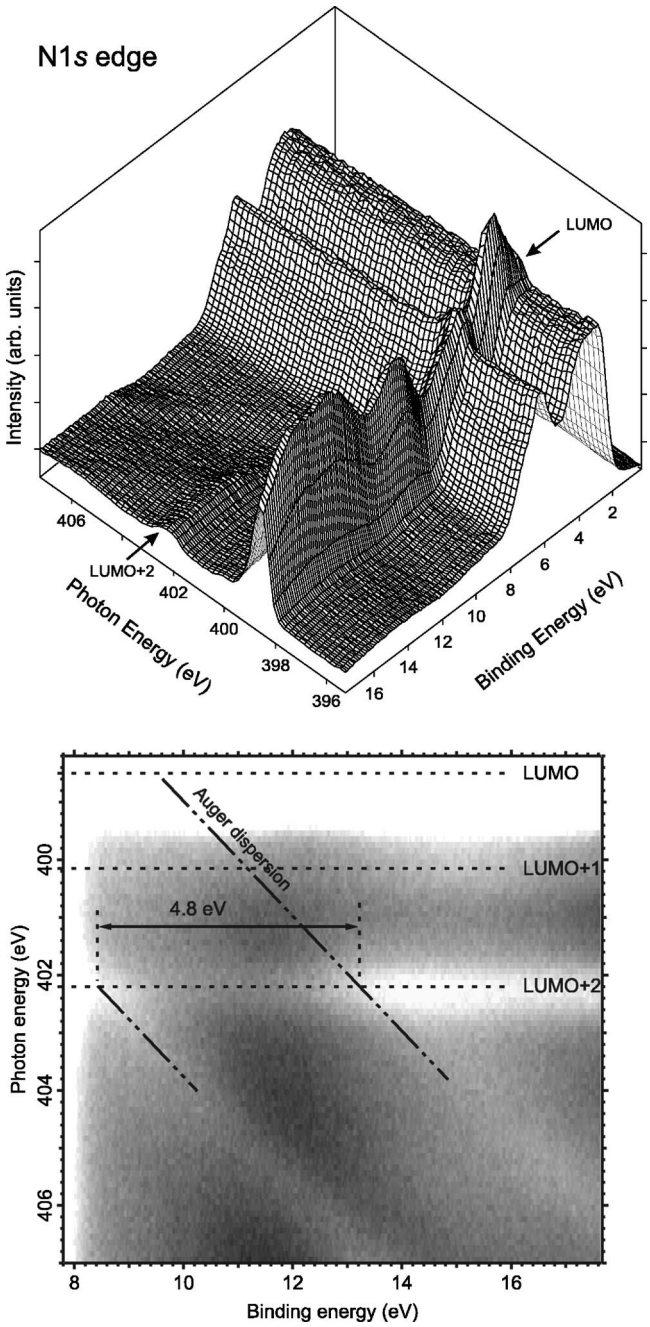


FIG. 7. Autoionization spectrum over the N 1*s* edge, for a monolayer of bi-isonicotinic acid on Au(111). Indicated are the positions of the LUMO, LUMO+1, and LUMO+2. Spectra were taken at normal emission. The sample was prepared using the cold technique. Photon resolution was ~100 meV, giving a binding energy resolution of ~760 meV.

Comparison of the participator signal of the molecule on Au(111) to that of a multilayer requires the two signals to be scaled to one another. Previous studies of the molecule on $TiO_2(110)$[6] scaled the participator-only signal relative to the NEXAFS signal (all deexcitation channels) through normalization of the spectra to the LUMO resonance. This resonance was used as, for a monolayer of bi-isonicotinic acid on $TiO_2(110)$, this unoccupied orbital is energetically coincident

with the substrate band gap; thus, no charge transfer can occur from or to it. The current energetic situation exhibited means that any quantitative information is limited by the applicability of the normalization procedure. This point will be returned to.

Previous studies of the molecule on $TiO_2$,[6] as well as an unpublished work of our own, shows that the majority of the electrons giving rise to the participator signal reside in a 5 eV BE window, starting at the onset of the highest occupied molecular orbital (HOMO). No electrons giving rise to the spectator signal enter into this region for these studies. Integration over this window (for each photon energy) gives a resonant photoemission spectra (unoccupied states as derived from electrons due to the participator decay only).

The present case has the additional consideration of a feature that tracks as an Auger-type signal. This is most obvious from ($h\nu$=402.0 eV, BE=8.0 eV) to ($h\nu$=407.0 eV, BE=13.0 eV). The feature is not observed for the clean surface ruling out the excitation of a Au Auger. Neither is it observed for a multilayer preparation. This would suggest its origin to be derived from the specific interaction between the molecule and the substrate. It is noted that this feature was always reproducible and could be seen for both the hot and cold monolayers. It is also noted that the width of the feature is very narrow for a typical Auger deexcitation. It is therefore tentatively suggested that this feature arises from the ultrafast charge transfer from substrate states located at the Fermi level into energetically overlapping LUMO states of the (core-excited) molecule. The feature is then due to a N Auger involving occupied LUMO states, motivating the appearance of the feature at a lower binding energy than the normal (i.e., involving valence states) N Auger. Further, its separation from the normal Auger is comparable to the separation of the molecule derived HOMO and LUMO states (see Fig. 7, bottom). Accordingly, this feature is termed here as a *superspectator*. Assuming such ultrafast backtransfer of charge would suggest a relatively strong coupling of the molecule to the substrate.

Experimentally, it is unclear whether the previously discussed superspectator feature tracks back into the LUMO region, due to the lack of states in the lower $\pi^*$ region. In extrapolating its trajectory to where it would enter into the LUMO, it is evident that a reduction in the window used to capture the participator signal must be made, to ensure that no spectator signal is present. This is at the expense of a higher level of noise. The effect of using a BE window that included electrons associated with spectator decay would result in an overintense participator-derived LUMO resonance. The LUMO+2 would be unaffected due to the dispersion behavior of the spectator signal. Normalization of the resonant photoemission data to the LUMO would then result in the LUMO+2 becoming too small as compared to the NEXAFS-derived signal, potentially rendering an inaccurate charge transfer identification. The window used to produce resonant photoemission plots was chosen as 1.8–5.3 eV. These results can be seen in Fig. 8. The prospect of backtransfer also opens the possibility of a new participator channel,[20] arising from participator decay in the presence of a second electron, that has transferred into the unoccupied

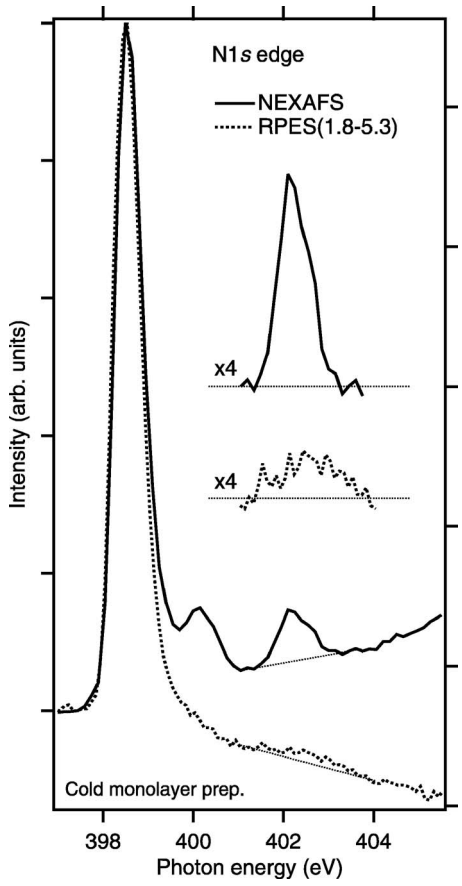


FIG. 8. N 1*s* RPES comparison to NEXAFS (all deexcitation channels). Spectra were normalized to the LUMO resonance. The resonant photoemission spectrum was derived by integration of electrons representing binding energies from 1.8 to 5.3 eV. Spectra were taken at normal emission. Photon energy resolution was ~100 meV. The sample was prepared using the cold technique.

orbitals from the substrate, in response to the creation of a core hole. This channel will be shifted due to the screening properties of this second electron. However, no evidence of two participator peaks in the resonant photoemission spectra has been found. This is unsurprising though, since the signal would be both small and not far shifted from the "usual" participator signal, making its resolution extremely difficult. Based on this and the relatively small intensity of the superspectator feature assigned to backtransfer, it is argued that any ultrafast backtransfer into the LUMO will not significantly affect its participator-derived size, and thus this point at least will not affect the validity of the normalization procedure applied to resonant photoemission spectra. In addition, the LUMO resonance has a slightly stronger overlap with the unoccupied substrate states.

The resonant photoemission spectrum derived from the data presented in Fig. 7, along with the sum of all deexcitation channels (NEXAFS), is shown in Fig. 8 for the cold monolayer preparation. Spectra were normalized to the LUMO resonance. The intensity of the LUMO+2 is reduced in the resonant photoemission data as compared to the NEXAFS. Some reduction is expected from matrix element effects.[6] Based on previous studies for a multilayer of biisonicotinic acid adsorbed on $TiO_2$(110),[6] the ratio between the two peaks is expected to be 1:0.33 in the absence of

charge transfer. The ratio found from the data in Fig. 8 is 1:0.34. This would suggest that no charge transfer occurs from the LUMO+2. This is not in contradiction with the suggested charge transfer from the substrate into the LUMO since coupling of the molecule to the substrate is specific to the orbitals involved. This has been shown theoretically for the cases of bi-isonicotinic acid on $TiO_2$(110) (Ref. 13) and pyridine on Au(111),[24] where orbital symmetry plays a key role. The apparent disappearance of the LUMO+1 would imply the opposite interpretation as given for the LUMO +2. However, its already low intensity in the NEXAFS prevents its use as a marker of charge transfer. It is noted that preliminary data for the hot preparation indicate the same resonant photoemission spectrum and hence the same conclusions.

Although it must be remembered that normalizing the resonant photoemission spectra to the LUMO is still in question in the current system (based on the energetics), any loss in intensity of the LUMO through any charge transfer out of it will not affect the presence of the LUMO+2, only its positive size, i.e., a reduction in the height of the LUMO results in a LUMO+2 too large in comparison with that of the NEXAFS, following normalization of spectra. Thus, any positive LUMO+2 signal indicates that femtosecond charge transfer does not occur for at least a fraction of molecules. Moreover though, it is argued that ultrafast charge transfer from the LUMO+2 does not occur for *all* molecules. The molecular orbitals involved, particularly with reference to those unoccupied (LUMO and LUMO+2), do not differ from those exhibited for multilayers of the molecule. Further to this, it has been shown that unoccupied orbitals exhibited by monolayers of the molecule adsorbed on $TiO_2$(110) also conform to the isolated molecule and multilayers of the molecule. It is therefore unlikely that the Au surface perturbs the molecular orbitals and as such, no change in the transition matrix elements associated with participator decay is expected. The ratio of 1:0.34 then suggests that the normalization procedure is correct and that the intensity of the participator LUMO+2 is at a maximum, with no molecules exhibiting ultrafast charge transfer from the LUMO+2 into the substrate.

## IV. CONCLUSIONS

In conclusion, it has been shown that the preparation technique employed in producing a monolayer of bi-isonicotinic acid on Au(111) will determine the type of monolayer formed. Independent of the preparations is the orientation of the aromatic ring structure. This was found to lie at an average tilt angle of $70° \pm 5°$ to the surface normal. Similarly independent was the lack of deprotonation upon molecule adsorption. Resonant photoemission data suggest the possibility of femtosecond charge transfer from the substrate to the molecule upon resonant excitation. No charge transfer is observed to occur from the LUMO+2 to the substrate as in previous studies of the molecule on $TiO_2$(110).[5,6] These results have significant implications for solar cell architectures based on a nanostructured $Au/TiO_2$ surface. Charge injection from molecules coupled to the oxide can occur on the low femtosecond time scale,[5] while charge transfer to the gold would be a much slower process. Moreover, gold can be used as a source of replenishing electrons with backdonation on the femtosecond time scale.

## ACKNOWLEDGMENTS

The authors are grateful for financial support by the European Community—Research Infrastructure Action under the FP6 "Structuring the European Research Area" Programme (through the Integrated Infrastructure Initiative "Integrating Activity on Synchrotron and Free Electron Laser Science"), the UK Engineering and Physical Sciences Research Council (EPSRC), Vetenskapsrådet, and the European Commission—through the Early Stage Researcher Training Network MONET. They also wish to give thanks to Sven Stoltz and Jesper Andersen for technical support during the beamtime.

[1] M. Grätzel and B. O'Regan, Nature (London) **353**, 737 (1991).
[2] A. Hagfeldt and M. Grätzel, Acc. Chem. Res. **33**, 269 (2000).
[3] B. A. Gregg and M. C. Hanna, J. Appl. Phys. **93**, 3605 (2003).
[4] L. Patthey, H. Rensmo, P. Persson, K. Westermark, L. Vayssieres, A. Stashans, Å Petersson, P. A. Brühwiler, H. Siegbahn, S. Lunell, and N. Mårtensson, J. Chem. Phys. **110**, 5913 (1999).
[5] J. Schnadt, P. A. Brühwiler, L. Patthey, J. N. O'Shea, S. Södergren, M. Odelius, R. Ahuja, O. Karis, M. Bässler, P. Persson, H. Siegbahn, S. Lunell, and N. Mårtensson, Nature (London) **418**, 620 (2002).
[6] J. Schnadt, J. N. O'Shea, L. Patthey, L. Kjeldgaard, J. Åhlund, K. Nilson, J. Schiessling, J. Krempaský, M. Shi, O. Karis, C. Glover, H. Siegbahn, N. Mårtensson, and P. A. Brühwiler, J. Chem. Phys. **119**, 12462 (2003).
[7] E. W. McFarland and J. Tang, Nature (London) **421**, 616 (2003).
[8] M. Grätzel, Nature (London) **421**, 586 (2003).
[9] R. Nyholm, J. N. Andersen, U. Johansson, B. N. Jensen, and I. Lindau, Nucl. Instrum. Methods Phys. Res. B **467–468**, 520 (2001).
[10] J. V. Barth, H. Brune, G. Ertl, and R. J. Behm, Phys. Rev. B **42**, 9307 (1990).
[11] J. Schnadt, J. Schiessling, J. N. O'Shea, S. M. Gray, L. Patthey, M. K. J. Johansson, M. Shi, J. Krempaský, J. Åhlund, P. G. Karlsson, P. Persson, N. Mårtensson, and P. A. Brühwiler, Surf. Sci. **540**, 39 (2003).
[12] J. Schnadt, J. N. O'Shea, L. Patthey, J. Schiessling, J. Krempaský, M. Shi, N. Mårtensson, and P. A. Brühwiler, Surf. Sci. **544**, 74 (2003).
[13] P. Persson, S. Lunell, P. A. Brühwiler, J. Schnadt, S. Södergren, J. N. O'Shea, O. Karis, H. Siegbahn, N. Märtensson, M. Bässler, and L. Patthey, J. Chem. Phys. **112**, 3945 (2000).
[14] J. Stöhr, *NEXAFS Spectroscopy* (Springer, Berlin, 1992).
[15] J. Stöhr and D. A. Outka, Phys. Rev. B **36**, 7891 (1987).
[16] J. N. O'Shea, Y. Luo, J. Schnadt, L. Patthey, H. Hillesheimer, J. Krempasky, D. Nordlund, M. Nagasono, P. A. Brühwiler, and N. Mårtensson, Surf. Sci. **486**, 157 (2001).
[17] J. N. O'Shea, J. B. Taylor, and E. A. Smith, Surf. Sci. **548**, 317 (2004).
[18] O. Björneholm, A. Nilsson, A. Sandell, B. Hernnäs, and N. Mårtensson, Phys. Rev. Lett. **68**, 1892 (1992).
[19] W. Wurth and D. Menzel, Chem. Phys. **251**, 141 (2000).
[20] P. A. Brühwiler, O. Karis, and N. Mårtensson, Rev. Mod. Phys. **74**, 703 (2002).
[21] A. Föhlisch, P. Feulner, F. Hennies, A. Fink, D. Menzel, D. Sanchez-Portal, P. Echenique, and W. Wurth, Nature (London) **436**, 373 (2005).
[22] J. Schnadt, J. N. O'Shea, L. Patthey, J. Krempaský, N. Mårtensson, and P. A. Brühwiler, Phys. Rev. B **67**, 235420 (2003).
[23] J. Schnadt, J. Schiessling, and P. A. Brühwiler, Chem. Phys. **312**, 39 (2005).
[24] S. Hou, J. Ning, Z. Shen, X. Zhao, and Z. Xue, Chem. Phys. **327**, 1 (2006).